Subharmonic bifurcations of standing wave lattices in a driven ferrofluid system

Hee-kyoung Ko, Jysoo Lee,* and Kyoung J. Lee†
National Creative Research Initiative Center for Neuro-dynamics and Department of Physics, Korea University, Seoul 136-701, Korea
(Received 22 January 2002; published 22 May 2002)

Superlattice standing waves arising on the surface of ferrofluids that are driven by an ac magnetic field are investigated experimentally. Several different types are obtained through successive spatial period doublings, which are mediated by resonant mode interactions. The observed superlattices are quite diverse, depending on the relevant base Fourier modes, the orientation and the number of emerged subharmonic modes, and the phase difference among the involved modes all together. On the other hand, their temporal evolutions are all either period-1 (harmonic) or period-2 (subharmonic).

DOI: 10.1103/PhysRevE.65.056222 PACS number(s): 05.45.−a, 05.65.+b, 89.75.−k

I. INTRODUCTION

Pattern formation in a spatially extended nonequilibrium system has been a subject of numerous studies during the last decade. Various laboratory and model systems are developed and characterized in different scientific disciplines [1]. Among others, perhaps the most important concern in these efforts has been to understand ''simple crystalline patterns'' that arise due to a single mode instability [1–4]. This is now a well established topic. Subsequently, an immediate question one might ask is if there are any generic routes along which the morphological complexity of a simple pattern increases in a systematic way. Much of the current research effort related to nonequilibrium pattern formation now lies on this venue of thought.

In many cases, one can view pattern forming nonequilibrium systems as a coupled network of nonlinear oscillators. Then, the morphological complexity of the pattern is expected to be related to the temporal dynamics of the constituent oscillators. Indeed, a series of recent model studies and laboratory experiments on different reaction-diffusion systems has shown that a subharmonic bifurcation of local oscillators in time domain can lead to a spatially period-doubled traveling wave state [5–8]. A number of such subharmonic bifurcations can then result in highly complex yet periodic patterns. In a different class of systems, however, such complex patterns can be induced not by the complexity of local dynamics but by resonant mode interactions. Pattern forming nonlinear systems are often able to generate different spatial modes simultaneously, and resonant interactions among these base modes can result in various complex-periodic lattice (superlattice) patterns. This different class of patterns is a subject of extensive current investigations [9–16].

In our earlier study, we showed that a resonant superlattice can be formed in a magnetically driven ferrofluid system [17]. The observed superlattice pattern arises in a bicritical situation in which a hexagonal lattice generated by the static Rosensweig instability [18] interacts with a subharmonic square lattice generated by the Faraday instability. Here, we demonstrate that sequences of such a resonant mode interaction can exhibit successive spatial subharmonic bifurcations as shown in Fig. 1. With a resonant mode interaction, a subharmonic mode emerges rendering a spatially ''period-doubled'' superlattice. As the control parameters are varied further, another subharmonic bifurcation takes place producing a more complex yet still periodic superlattice. As it will be demonstrated, the morphology of the resulting superlattice can be quite diverse depending on the involved base wave vectors, the orientation and number of the emerged (primary and secondary) subharmonic modes, and the phase difference among the selected Fourier modes. The temporal dynamics of the observed superlattices are, however, either harmonic or subharmonic, unlike the case of complex oscillatory media, in which the spatial and temporal complexities increase or decrease simultaneously.

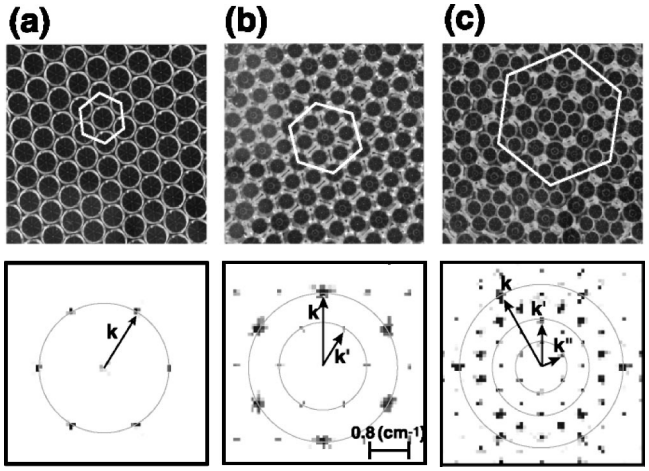

FIG. 1. Successive spatial period doublings of a hexagonal lattice: (a) harmonic hexagon $1h(f=6.20$ Hz, $\Delta H=0.17H_c)$; (b) spatially period-2 harmonic superlattice $2h(f=5.60$ Hz, $\Delta H=0.50H_c)$; and (c) spatially period-4 subharmonic superlattice $4H(f=6.06$ Hz, $\Delta H=0.42H_c)$ are shown at the top row. H_c $(=108.0$ G) is the critical field of the static Rosensweig instability. Each frame is $61\times61\text{mm}^2$. Each hexagonal tiling unit is guided by white line. The corresponding Fourier modes are shown at the bottom row.

*Present address: Supercomputing Center, Korea Institute of Science and Technology Information, P.O. Box 122, Yusong, Daejon 305-806, Korea.

†Author to whom correspondence should be addressed; electronic address: kyoung@nld.korea.ac.kr.

II. EXPERIMENT

The patterns are observed in a magnetically driven Faraday system employing ferrofluids [17,19,20]. Ferrofluids are a colloidal suspension of magnetic powder stabilized by screened electrostatic repulsion [18]. Unless specified otherwise, 1:1 mixture of commercially available ferrofluids (EMG901 and EMG909, Ferrofluidics) are used. The physical properties of EMG901 (EMG909) are, density $\rho = 1.53$ (1.02)g/ml, surface tension $\sigma = 27.5$ (27.5)g/s^2, initial magnetic susceptibility $\chi = 3.00$ (0.80), magnetic saturation $M_s = 600$ (200)G, and dynamic viscosity $\eta = 10$ (6) CP, yielding a critical field of static Rosensweig instability 90.5 (168.2)G, respectively. A cylindrical Teflon container containing the ferrofluid (fluid depth = 1.16 mm, container depth = 50 mm, and inner diameter = 140 mm) is placed in the center of a pair of Helmholtz coils with an inner (outer) diameter of 200 mm (280 mm). The distance between two coils is 120 mm. The magnetic field is monitored by a hall probe (F. W. Bell Inc., Model 6010), and the spatial variation of the field strength is within 3% in the monitored area. An ac signal is generated from a home-built synthesizer board and amplified by a linear amplifier driving the total magnetic field of $H(t) = H_0 + \Delta H \sin(2\pi f t)$. H_0 is the static field, ΔH is the amplitude of ac component, and f is the driving frequency. H_0 is fixed at 0.93 H_c for all cases, while ΔH and f are used as control parameters. The temperature of the container is maintained at 15 °C.

The fluid surface is illuminated by three arrays of concentric light-emitting diode rings (diameters 160, 180, and 200 mm, respectively) located 275 mm above the surface. The patterns are imaged at a resolution of 530×512 pixels using a charged-coupled device camera (Quantix, Photometrics) located 560 mm above the surface with a frame grabber (Meteor2/DIG, Metrox) in stroboscopic modes with an exposure time of 3 ms. The flat surfaces either above or below the level of surrounding fluid appear white, while the nonflat surfaces that scatter the light away from the camera appear black.

III. HEXAGON-BASED SUPERLATTICES

A good example of successive spatial period doublings is shown in Fig. 1. Figure 1(a) shows a temporally harmonic hexagonal standing wave pattern ($1h$, the nomenclature is given in Ref. [21]) and the associated six Fourier peaks ($\vec{k}$). This pattern, which forms in a vicinity of the Rosensweig (static) instability, is simply periodic both in space and time. As the driving amplitude and frequency are increased, however, the $1h$ pattern undergoes a subharmonic bifurcation resulting in a spatially period-doubled hexagonal superlattice ($2h$) as shown in Fig. 1(b). The magnitude of the newly emerged six subharmonic wave vectors ($\vec{k}'$), that are rotated 30° relative to the six base modes ($\vec{k}$), are $\sqrt{3}$ times smaller than the original base wave vectors. The $2h$ pattern is still harmonic in time.

As the driving frequency increases, the $2h$ superlattice undergoes another subharmonic bifurcation in space [see Fig. 1(c)] — a set of six secondary subharmonic modes ($\vec{k}''$) appears in addition to the base modes ($\vec{k}$) and the six primary subharmonics ($\vec{k}'$), thus forming a spatially "period-4" hexagonal superlattice ($4H$). Unlike the case of the first subharmonic bifurcation, the secondary subharmonic wave vectors are twice smaller than those of the primary subharmonics, lining up with the primary subharmonics. The $4H$ superlattice is temporally subharmonic. The underlying mechanism for the observed spatial subharmonic bifurcations is believed to be resonant mode interactions.

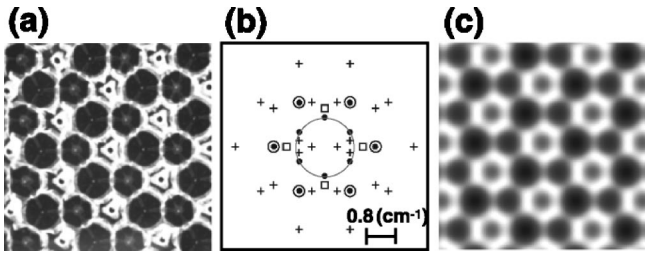

FIG. 2. Generation of $2H$ hexagonal superlattice by resonant triadal interaction: (a) snapshot of $2H$ pattern ($f = 8.00$ Hz, $\Delta H = 0.25 H_c$, field of view $= 44 \times 44$mm^2); (b) twelve modes of $2H$ [●, measured from (a) directly; for clarity, only the positions of the Fourier vectors are marked], six harmonic hexagonal modes of $1h$ (○, obtained from Fig. 3), four subharmonic square modes of $1S_1$ (□, obtained from Fig. 3), and some elementary modes generated by triadal interactions (+) between $1h$ and $1S_1$; and (c) reconstructed image based on the twelve measured modes of $2H$(●).

Let us first discuss the resonant mode interaction resulting in a hexagonal superlattice $2H$ pattern that is shown in Fig. 2(a). The $2H$ originates from a resonant triadal interplay between harmonic hexagonal modes of $1h$ and subharmonic square modes of $1S_1$. As shown in Fig. 2(b), of the total 12 relevant Fourier modes of $2H$ ("●") six outer peaks exactly overlap with the basic Fourier modes of $1h$(○). The six Fourier modes of $1h$ are obtained by linearly extrapolating the empirically measured dispersion relation shown in Fig. 3. Similarly, the four Fourier modes of $1S_1$ (□) are obtained from Fig. 3. The inner subharmonic peaks of $2H$ (six points marked by "●" lying along the circle) have two different origins. The two points lying along the k_y axis are neighbor-

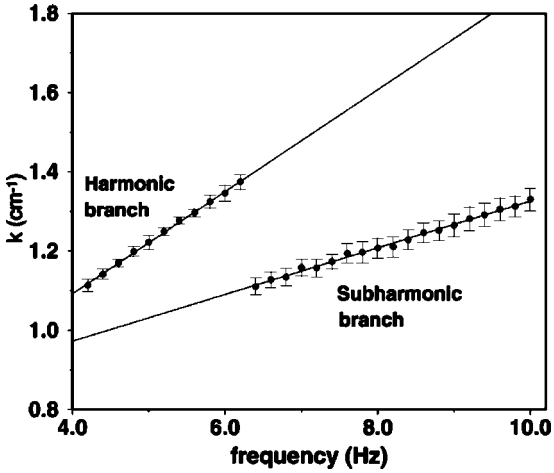

FIG. 3. Dispersion relation measured for $\Delta H = 0.15 H_c$.

ing a Fourier peak of $1S_1$ (open square) very closely. Thus, most likely they originate from $1S_1$ lattice. On the other hand, each one of the four remaining inner peaks are closely located to a resonant mode $(+)$ of $1h$ and $1S_1$. Here, in particular, the relevant resonant modes are the ones satisfying $\vec{k}_+ = \vec{k}_\bigcirc - \vec{k}_\square$. Since the $2H$ pattern involves the Fourier modes of $1S_1$ lattice, it naturally has a subharmonic oscillation in time as a whole.

Figure 2(c) is a reconstructed Fourier image purely based on the measured twelve Fourier vectors of $2H$ ["●" in Fig. 2(b)]. The image captures the three different cell types that are present in Fig. 2(a). The relative phase difference between the harmonic and subharmonic modes turns out to be quite important in determining the morphology of the concerned superlattice. The phase difference of $\pi/2$ is required in order to achieve a hexagonal superlattice that has three different cell types. If the phase difference between the harmonic and subharmonic modes is zero, only two different cell types exist as in the case of $2h$.

Although the $2h$ pattern has almost the same Fourier spectrum of $2H$ as shown in [Fig. 1(b)], it is different from $2H$ in several aspects: (1) $2H$ is subharmonic in time, while $2h$ is harmonic; (2) the six subharmonic Fourier peaks of the $2h$ pattern cannot be obtained by the same triadal interaction of $1h$ and $1S_1$ modes that resulted the $2H$ pattern; (3) $2H$ is observed in a "small amplitude forcing regime" while $2h$ is observed in a "large amplitude forcing regime." These differences all together suggest that the $2h$ pattern does not arise by a simple resonant triadal interaction but by a higher order resonant interaction beyond the three-wave interaction. Since there are so many possible resonant modes at higher-order regime, it is currently beyond our limit to discuss exactly which resonant modes are participating in the $2h$ pattern. The fact that the $2h$ pattern has a simple harmonic oscillation also excludes any possible connection to a higher-order resonant tongue associated with the Faraday instability (e.g., $3f/2$ tongue). Similarly, the observed $4H$ pattern would be explained only by a higher-order resonant interaction. In fact, the $2h$ and $4H$ patterns are observed in a large amplitude regime in which high-order resonant interactions would become important.

IV. SQUARE-BASED SUPERLATTICES

Similar spatial subharmonic bifurcations are also observed in a square lattice as well. Figure 4 shows three different square superlattices $2S_a$, $2S_i$, and $4S_a$ formed by resonant mode interactions. The temporally subharmonic square standing wave $1S_1$ undergoes a spatial subharmonic bifurcation to either $2S_a$ [Fig. 4(a)] or $2S_i$ [Fig. 4(b)], as the system is brought into a large amplitude regime. Only a pair of subharmonic wave vectors newly appears along one of the two symmetric axes of the preexisting four base vectors for *anisotropic* $2S_a$, while two pairs of subharmonics appear simultaneously for *isotropic* $2S_i$. Consequently, $2S_a$ is spatially period-doubled only in one direction (y axis for the given example), whereas $2S_i$ is doubled in both x and y directions. The transition between two neighboring states $2S_a$ and $2S_i$ is found to be continuous. In other words, the additional pair of subharmonic modes along k_x axis gradually appears from $2S_a$ pattern rendering $2S_i$ pattern, as the driving frequency or amplitude is increased [22].

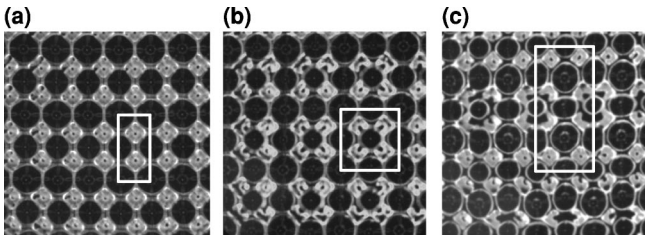

FIG. 4. Successive spatial period doublings of a square lattice. The simple subharmonic square $1S_1$ (not shown) bifurcates to either (a) spatially period-2 *anisotropic* square $2S_a(f=6.52$ Hz, $\Delta H=0.30H_c)$ or (b) spatially period-2 *isotropic* square $2S_i(f=7.00$ Hz, $\Delta H=0.30H_c)$. (c) The $2S_i$ superlattice further bifurcates to spatially period-4 *anisotropic* square $4S_a(f=7.00$ Hz, $\Delta H=0.29H_c)$. Each frame is 44×44 mm^2. Each square (or rectangular) tiling unit is guided by white line.

When the system is moved further from $2S_i$ to a higher-frequency regime, an additional doubling occurs resulting in the $4S_a$ pattern shown in Fig. 4(c). The complex square superlattice $4S_a$ has total ten Fourier modes including four base vectors of $1S_1$, four primary subharmonics of $2S_i$, and a new pair of secondary subharmonics along one of the two principal axes. This additional pair is exactly half the size of the preexisting primary subharmonics. Thus, the x-y symmetry is lost in $4S_a$ as in the case of $2S_a$. In our current experimental condition, no isotropic $4S$ superlattice has been found.

Careful analysis on the Fourier modes of all three square superlattices $2S_a$, $2S_i$, and $4S_a$ has been carried out in conjunction with all possible triadal resonant interactions between the modes of two basic lattices $1h$ and $1S_1$. The agreements between the observed modes and the modes generated by triadal mode interactions turn out to be poor for the primary subharmonics of $2S_a$ and $2S_i$, and worse for the secondary subharmonics of $4S_a$. In other words, these square-based superlattices do not originate from triadal mode interactions. We believe that they arise with higher-order resonant interactions between $1h$ and $1S_1$

V. OTHER PATTERNS AND PHASE DIAGRAM

The spatial periodicity of 4 is the highest thus achieved so far, but in principle, the doubling cascade can go on further as the number of modes participating in the resonant interaction increases. On the contrary, some of the high-order resonant mode interactions can produce simple lattice patterns as well. A good example is the subharmonic square lattice $1S_2$ observed in a large amplitude regime. Although it is identical to the $1S_1$ pattern in all aspects, its Fourier modes have a quite different origin — none of its four wave vectors match the wave vectors of $1h$, $1S_1$, or the ones created by triadal interactions between them. This is also true for the harmonic rhombus $1r$ also observed in a large amplitude regime.

The phase diagram shown in Fig. 5 summarizes

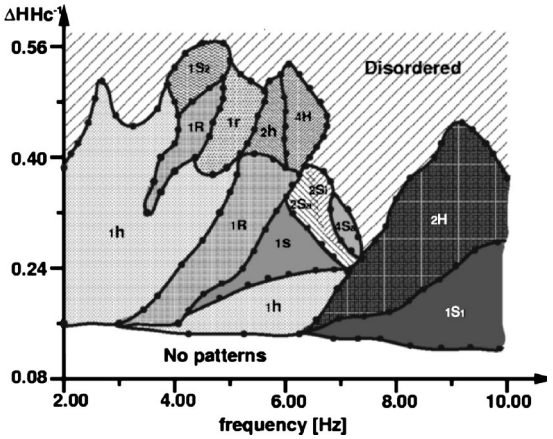

FIG. 5. Phase diagram of standing wave patterns revealed in a magnetically driven ferrofluid with $H_0=0.93\ H_c$. All together, six different superlattices ($2h$, $2H$, $4H$, $2S_i$, $2S_a$, $4S_a$) and six different simple lattices ($1h$, $1s$, $1S_1$, $1S_2$, $1r$, $1R$) are observed. The nomenclature of the observed patterns is described in Ref. [21].

the rich variety of observed patterns and their relative locations—all together *twelve* different types are revealed. In addition to the ones discussed earlier, simple harmonic square lattice $1s$ and subharmonic rhombus $1R$ are also observed in a small amplitude regime. The $1R$ forms with conventional triadal interaction [23]. The $1s$ pattern neighboring $1h$ is very similar to the ones discussed in previous reports [10,12]. The transitions between two neighboring patterns are all hysteretic [24] except for the one between $2S_a$ and $2S_i$, which is continuous as described earlier. The overall structure of the phase diagram depends quite sensitively on the property of the used ferrofluid. For a comparison, we have conducted the same experiment with 2:1 mixture of EMG901 and EMG909 to find no superlattice whatsoever, and with EMG901 only to find a superlattice of the $2H$ type. Nevertheless, the two basic competing lattices, $1h$ and $1S_1$, are both present in all three different cases. In other words, the two primary instabilities are not is sensitive to the property of the fluid, but the resonant mode interactions are.

VI. CONCLUSION

We have investigated superlattice standing wave patterns that arise on the surface of parametrically driven ferrofluids. All together, six different superlattices along with six different simple lattice patterns are observed. It is significant that all the observed superlattices arise through spatial subharmonic bifurcations mediated by resonant mode interactions. A similar spatial period-doubling phenomenon is reported earlier in the context of traveling waves of complex oscillatory media [5,8], but here it is discussed in the context of standing waves and resonant mode interaction. The observed superlattices are temporally simple (either harmonic or subharmonic to the forcing), again in good contrast to the complex periodic traveling waves that are complex oscillatory in time as well. Our experimental results raise a number of new theoretical issues such as (1) why the subharmonic modes of the base wave vectors are so much preferred by resonant interactions over various other possible resonant modes, and (2) what would be the maximum spatial complexity that can be achieved by resonant mode interaction under a given condition. Full understanding of the rich variety of standing wave patterns and their mutual boundaries also pose quite a challenge.

ACKNOWLEDGMENT

This work was supported by the Creative Research Initiatives of the Korean Ministry of Science and Technology.

[1] See, e.g., M. Cross and P. Hohenberg, Rev. Mod. Phys. **65**, 851 (1993).
[2] Q. Ouyang and H.L. Swinney, Nature (London) **352**, 610 (1991).
[3] F. Melo, P. Umbanhowar, and H.L. Swinney, Phys. Rev. Lett. **75**, 3838 (1995).
[4] S.W. Morris, E. Bodenschatz, D.S. Cannell, and G. Ahlers, Phys. Rev. Lett. **71**, 2026 (1993).
[5] A. Goryachev and R. Kapral, Phys. Rev. Lett. **76**, 1619 (1996).
[6] A. Goryachev, H. Chaté, and R. Kapral, Phys. Rev. Lett. **80**, 873 (1998).
[7] A. Goryachev, H. Chaté, and R. Kapral, Phys. Rev. Lett. **83**, 1878 (1999).
[8] J.-S. Park and K.J. Lee, Phys. Rev. Lett. **83**, 5393 (1999).
[9] W.S. Edwards and S. Fauve, J. Fluid Mech. **278**, 123 (1994); Phys. Rev. E **47**, R788 (1993).
[10] A. Kudrolli, B. Pier, and J.P. Gollub, Physica D **123**, 99 (1998).
[11] H. Arbell and J. Fineberg, Phys. Rev. Lett. **81**, 4384 (1998).
[12] H. Arbell and J. Fineberg, Phys. Rev. Lett. **84**, 654 (2000).
[13] H. Arbell and J. Fineberg, Phys. Rev. Lett. **85**, 756 (2000).
[14] C. Wagner, H.W. Müller, and K. Knorr, Phys. Rev. Lett. **83**, 308 (1999).
[15] C. Wagner, H. W. Müller, and K. Knorr, e-print patt-sol/9911001.
[16] M. Silber and M.R.E. Proctor, Phys. Rev. Lett. **81**, 2450 (1998); M. Silber and A.C. Skeldon, Phys. Rev. E **59**, 5446 (1999).
[17] H.-J. Pi, S.-y. Park, J. Lee, and K.J. Lee, Phys. Rev. Lett. **84**, 5316 (2000).
[18] R. Rosensweig, *Ferrohydrodynamics* (Cambridge University Press, Cambridge, England, 1985).
[19] J.-C. Bacri, U. d'Ortona, and D. Salin, Phys. Rev. Lett. **67**, 50 (1991).
[20] T. Mahr and I. Rehberg, Europhys. Lett. **43**, 23 (1998).
[21] The following nomenclature is used for labeling diverse patterns observed in our system. The leading *numbers* $1=2^0$, $2=2^1$, and $4=2^2$ represent the base state, subharmonic state, and sub-subharmonic state, respectively. The subsequent alphabet represents the symmetry of the involved lattice (e.g., *H*

represents hexagon, *S* represents square, and *R* represents rhombus) and the temporal behavior (small letter: harmonic in time to the magnetic ac forcing, capital letter: subharmonic to the forcing). The following additional subscripts are used when necessary (*i* for isotropic, *a* for anisotropic, 1 for 1st kind, and 2 for 2nd kind).

[22] Since the acquired full image is not sufficiently large to reveal the subharmonic Fourier peaks clearly, we quantified this transition by directly measuring the ratio (m) of two different cell sizes along the x axis. The order parameter m decays continuously from $2S_i$ to $2S_a$. The driving frequency f is varied while maintaining $\Delta H = 0.30 H_c$.

[23] Our $1R$ pattern has the same origin of the ''two-mode rhomboid'' ($2k$R) pattern described in Ref. [12] except that all four Fourier modes of the $1R$ pattern are resonant modes whereas only two out of four are such for the $2k$R pattern.

[24] The bistable ranges are typically an order of $\delta f = 0.1$ Hz and $\delta [\Delta H/H_c] = 0.02$.